

Characteristics of MoO₃ Reduced with H₂ at the Different Flow Rates of H₂

Takeshi Matsuda,* Yasuyoshi Hirata, Fumiko Uchijima, Hidenobu Itoh, and Nobuo Takahashi

Department of Materials Science, Kitami Institute of Technology, Koen-cho 165, Kitami, Hokkaido 090-8507

(Received October 4, 1999)

MoO₃ was treated with H₂ at 623 K for 12 h. The degree of reduction and the specific surface area of H₂-reduced MoO₃ were dependent on the flow rate of H₂ in the reduction process. MoO₃ with a surface area of about 5 m² g⁻¹ was transformed to a porous MoO_x with a surface area of 180 m² g⁻¹ after reduction at a flow rate of H₂ larger than 600 ml min⁻¹ g⁻¹. The MoO_x was found to be stable at 623 K, even in the presence of H₂O vapor. A study of reduction with a mixture of H₂ and H₂O showed that the degree of reduction and the surface area decreased with increasing partial pressure of H₂O in the reduction process. We conclude from these results that the reduction of MoO₃ to porous MoO_x with a large surface area was prohibited by the action of H₂O produced by the reduction.

Micro and mesoporous inorganic materials have found to be a great utility as catalysts and absorbents due to their large internal surface. Typical microporous materials are zeolites. Zeolites and related crystalline molecular sieves possess not only catalytically active sites, but also uniformly sized pores, which allow their industrial application as shape-selective catalysts. Since the discovery of MCM-41 by Mobil Oil Corporation,^{1,2} the preparation of nanostructured porous materials has attracted great interest in materials science. The synthesis and characteristics of Si-based micro and mesoporous materials have been extensively investigated by many research groups. Although the preparation of mesoporous transition metal oxides from a cooperative assembly of a periodic inorganic and surfactant-based structure has recently been reported,^{3,4} there have been few studies concerning microporous transition metal oxides. Nanostructured transition metal oxides are expected to have some advantages over Si-based materials for applications in electromagnetics, photoelectronics, and catalysis because transition metals can exist in various oxidation states.

Mo is an important catalytic component, and its physical and catalytic properties have been investigated in detail. In practice, Mo-based materials have been used as catalysts for the hydrodesulfurization of petroleum feed stocks and the selective oxidation of alkenes in industrial processes. Unique catalytic functions of Mo-based materials have recently been reported. Katrib and co-workers^{5,6} showed by systematic studies using catalytic reactions in association with spectroscopic techniques that the MoO₂ phase was capable of catalyzing the isomerization of alkane without cyclization and excessive hydrocracking. It was shown in our previous papers⁷⁻⁹ that MoO₃ reduced with H₂ at 623 K was active for the isomerization of heptane and for the dehydration and dehydrogenation of 2-propanol. After reduction for 48 h, MoO₃ exhibited high dehydration activity compared with

that of zeolite catalysts. The H₂ reduction of MoO₃ at 623 K was accompanied by an increase in the surface area: the MoO₃ reduced for 12 h or longer had a surface area of 180 m² g⁻¹. Furthermore, reduced MoO₃ with a large surface area was found to have micropores, of which the diameter was in the range from 6 to 30 Å.¹⁰ We showed in a previous paper¹¹ that the catalytic activities for the conversions of heptane and 2-propanol and the surface area of H₂-reduced MoO₃ were markedly affected by the flow rate of H₂ in the reduction process. The main purpose of the present work is to describe the effect of the flow rate of H₂ in the reduction process on the transformation of MoO₃ to MoO_x with a large surface area.

Experimental

H₂ and N₂ were purified by passing through a molecular sieve and a Mn/SiO₂ oxygen trap. The MoO₃ used in this study was obtained by calcination of H₂MoO₄·H₂O (Kanto Chemical Inc.) at 673 K for 3 h. The powder was made into pellets, crushed, and then sieved (30–60 mesh) for charging into a cell.

A prescribed amount of MoO₃ (0.1–0.5 g) was packed at the central position of a cell, which was made of a pyrex glass tube with an inner diameter of 6 mm. The sample was heated to 623 K at a rate of 5 K min⁻¹ in a stream of H₂, and was kept for a desired period, typically for 12 h. The flow rate of H₂ was varied from 60 to 1200 ml min⁻¹ g-MoO₃⁻¹. The reduced MoO₃ samples are denoted here by MoO₃ (60), MoO₃ (1200), etc. The values in parentheses represent the flow rate of H₂ in the reduction process. Water vapor was added to the gas stream by passing H₂ or N₂ through a water saturator in a constant temperature bath.

The surface area was determined from a N₂ adsorption isotherm, which was obtained on the sample without exposure to air. The reduced sample was cooled to room temperature with H₂ still flowing. After evacuation for 0.5 h at room temperature, the adsorption of N₂ was measured at 77 K using a conventional high-vacuum static system. To determine the pore-size distribution, adsorption-desorption isotherms of N₂ were measured with an automatic gas-

adsorption apparatus (Sorpomatic 1990, Carlo Erba) after evacuation at 573 K for 2 h. Pore-size distribution curves were obtained by analyzing the adsorption data using the Horvath-Kawazoe method.

The average oxidation state of Mo was determined by measuring the amount of O₂ consumption required for complete reoxidation to MoO₃ after the reduction procedure. A pulse technique was employed. The procedures for reoxidation were described in detail elsewhere.⁹

Crystalline phases of H₂-reduced MoO₃ were determined by X-ray diffraction using Ni-filtered Cu K α radiation. The sample for XRD measurements was obtained as follows: MoO₃ was subjected to H₂ reduction at 623 K for 12 h, followed by flowing N₂ for 0.5 h at the same temperature. After cooling to room temperature under a N₂ atmosphere, the sample was passivated for 1 h with a 1% O₂-99% N₂ gas mixture to avoid any strong bulk oxidation.

Results and Discussion

We showed in a previous paper⁹ that the physical and catalytic properties of MoO₃ were dependent on the period of H₂ reduction at 623 K: The catalytic activities for the conversions of heptane and 2-propanol and the surface area increased for longer periods of reduction. It was found that the surface area of H₂-reduced MoO₃ was affected not only by the reduction period, but also by the flow rate of H₂. Figure 1 shows the surface area of reduced MoO₃ as a function of the flow rate of H₂ in the reduction process, which was performed at 623 K for 12 h. The parent MoO₃ had a surface area of about 5 m² g⁻¹. H₂ reduction enlarged the surface area remarkably. A change in the surface area was induced when the reduction condition differed only in the flow rate of H₂. The surface area increased in proportion to the flow rate of H₂, and reached a constant value of about 180 m² g⁻¹ at a flow rate of H₂ larger than 600 ml min⁻¹ g⁻¹. XRD patterns of the MoO₃ reduced for 12 h are demonstrated in Fig. 2. The diffraction lines corresponding to the MoO₃ phase completely disappeared after reduction for 12 h, irrespective of the flow rate of H₂. MoO₃ (60) provided only the diffraction

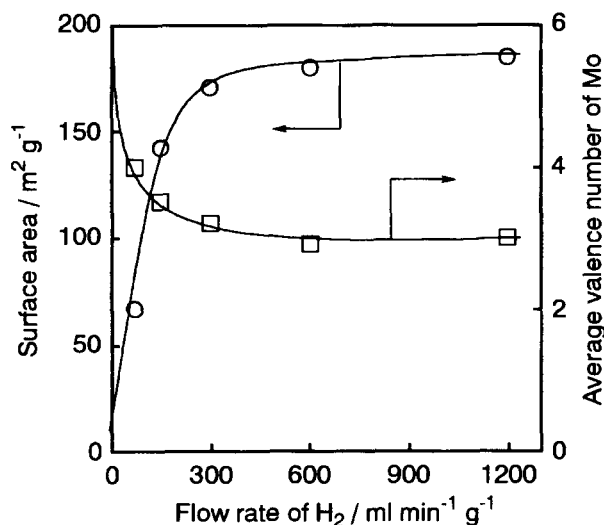


Fig. 1. Effect of the flow rate of H₂ in the reduction process on the surface area of reduced MoO₃. MoO₃ was reduced at 623 K for 12 h.

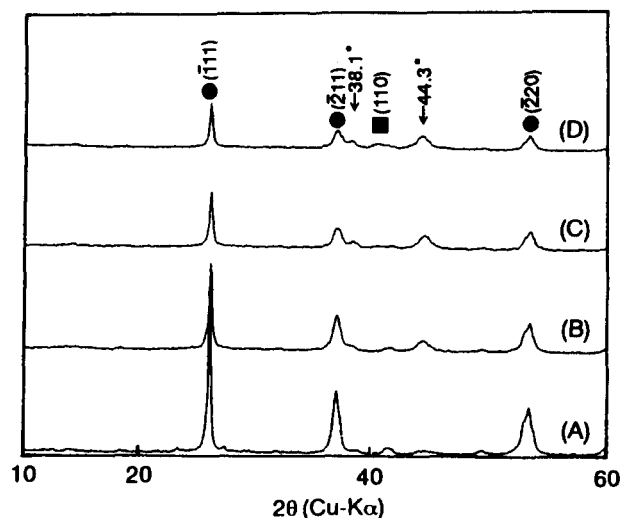


Fig. 2. XRD patterns of MoO₃ reduced with H₂ at 623 K for 12 h. Flow rate of H₂/ml min⁻¹ g⁻¹: (A), 60; (B), 300; (C), 600; (D), 1200. ●, MoO₂; ■, Mo metal.

lines corresponding to the MoO₂ phase. The intensity of these peaks was weakened by an increase in the flow rate of H₂, after which new peaks appeared at $2\theta = 38.1^\circ$ and 44.3° . In the case of MoO₃ (1200), the $d(110)$ diffraction of Mo metal was observed at $2\theta = 40.5^\circ$. As shown in Fig. 1, MoO₃ was more deeply reduced at a larger flow rate of H₂. This is in accordance with the XRD results.

Hydrogen molybdenum bronze, H₂MoO₃, provides the diffraction line of $d(600)$ at 40.0° . This line appears at a lower angle when the content of H₂ decreases: the $d(600)$ diffraction line of H_{0.93}MoO₃ is observed at $2\theta = 37.2^\circ$. Thus, the diffraction line appearing at $2\theta = 38.1^\circ$ seems to be related to hydrogen molybdenum bronze, H_xMoO₃. Delporte and co-workers¹² showed that a treatment of MoO₃ with a mixture of H₂ and hydrocarbon at 623 K yielded molybdenum oxycarbide, MoO_xC_y, where carbon atoms were substituted for some of oxygen atoms. This phase gave the diffraction line at $2\theta = 44.3^\circ$. They stated that H or H₂ was able to act like C atoms to form MoO_xH_y, of which the diffraction line appeared at $2\theta = 44.5^\circ$. We deduce from the reported results that the line at $2\theta = 44.3^\circ$ reflected the formation of the MoO_xH_y phase.

The surface area of MoO₃ has already been reported to be enlarged in a temperature-programmed reaction with NH₃,^{13,14} in carburization under a H₂ and CH₄ mixture,¹⁵⁻¹⁷ and in H₂ reduction.¹² The following mechanism has been proposed to explain this phenomenon:¹⁸ The reduction of MoO₃ begins preferentially at the shear planes, which are crystallographic defects created by the aggregation of oxygen vacancies to form planes of molybdenum bound to a tetrahedron of oxygen atoms instead of the octahedrally bound molybdenum of bulk MoO₃. As reduction proceeds in these planes, the metal lattice contracts and fractures the crystal to generate a large surface area.

According to this mechanism, reduction at the larger flow rate of H₂ provides smaller particles. Hence, the particle size

of the reduced MoO_3 was calculated from the $d(\bar{1}11)$ line of the MoO_2 phase using the Sherrer equation. The results are given in Table 1. Particles of the parent MoO_3 had an average size of about 500 Å which was determined from the $d(020)$ diffraction line of the MoO_3 phase. The size of the produced MoO_2 particles was small compared with that of the parent MoO_3 . This is consistent with the reported results. The particle size of MoO_2 , however, increased in proportion to the flow rate of H_2 . The surface area was calculated from the particle size by assuming spherical particles. The calculated surface areas of reduced MoO_3 were much smaller than the surface areas determined from the adsorption isotherms of N_2 . These results indicate that the enlargement of the surface area cannot be attributed to the formation of MoO_2 particles with smaller size. A treatment of MoO_3 with a mixture of H_2 and hexane at 623 K was reported to produce a mixture of MoO_2 and MoO_xC_y phases, of which the surface area was about $150 \text{ m}^2 \text{ g}^{-1}$.¹² As mentioned above (Fig. 2), H_2 -reduced MoO_3 with a large surface area gives a diffraction line at $2\theta = 44.3^\circ$, while that with a small surface area, such as $\text{MoO}_3(60)$, does not. We deduce from these results that the large surface area of H_2 -reduced MoO_3 is related to the formation of the MoO_xH_y phase.

The type of N_2 adsorption isotherm was found to be dependent on the flow rate of H_2 . The BET isotherm gave a better fit of the N_2 adsorption data on the parent MoO_3 and $\text{MoO}_3(75)$ than the Langmuir isotherm. For reduced MoO_3 with large surface areas, such as $\text{MoO}_3(600)$, however, the Langmuir equation provided a satisfactory linear fit of the N_2 adsorption data, while the BET did not. These results suggest the presence of micropores in the reduced MoO_3 with large surface areas. In order to confirm this, N_2 adsorption-desorption isotherms and the corresponding pore size distribution curves were determined. Figure 3 shows the adsorption-desorption isotherms of N_2 on $\text{MoO}_3(75)$ and $\text{MoO}_3(600)$. $\text{MoO}_3(600)$ gave no hysteresis, and the amount of N_2 adsorption increased sharply at very low pressures, and changed little at intermediate pressures. These phenomena are characteristics of microporous materials. In contrast, the amount of N_2 adsorption on $\text{MoO}_3(75)$ increased slightly in keeping with the pressure. Pore-size distribution curves determined by the Horvath-Kawazoe method are demonstrated in Fig. 4. $\text{MoO}_3(600)$ was found to possess micropores, of which the diameter was in the range from 6 to 30 Å. The value of Dv/Dr was enlarged by an increase in the flow rate of H_2 , suggesting the progression of a porous structure. It is obvious from these results that the reduction of MoO_3 at the larger flow rate of H_2 yielded a microporous MoO_x with

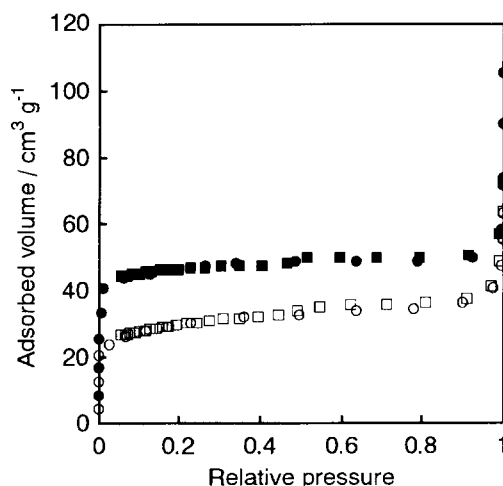


Fig. 3. Adsorption-desorption isotherm of N_2 on MoO_3 reduced at 623 K for 12 h. Flow rate of $\text{H}_2/\text{ml min}^{-1} \text{ g}^{-1}$: open symbols, 75; solid symbols, 600. Isotherm: circles, adsorption; squares, desorption.

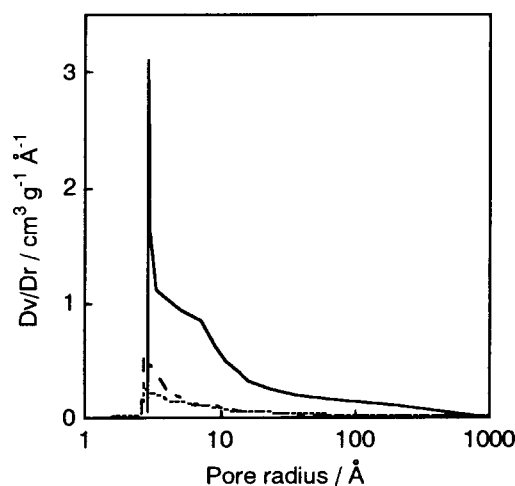


Fig. 4. Pore size distribution in MoO_3 reduced at 623 K for 12 h. Flow rate of $\text{H}_2/\text{ml min}^{-1} \text{ g}^{-1}$: ····, 75; ---, 150; —, 600.

a larger surface area. The large surface area of H_2 -reduced MoO_3 seems to be caused by the formation of micropores. We reported in a previous paper that the surface area and porosity of the reduced MoO_3 were dependent on the period of H_2 reduction.¹⁰ The effect of the H_2 flow rate on the characteristics of reduced MoO_3 are very similar to that of the reduction period.

It was reported that Mo_2N with a larger surface area was produced at a greater space velocity of NH_3 in a temperature-programmed reaction of MoO_3 and NH_3 .^{18,19} The resultant high surface area was achieved only when the reaction took place at a slow, controlled rate, so that oxygen could be removed and replaced with nitrogen without any substantial reorganization of the metal lattice. The concentration gradient of NH_3 in a MoO_3 bed was thus suggested to affect the surface area of the resultant Mo_2N . The importance of the space velocity was also stated in the synthesis of Mo_2C by the temperature-programmed reduction of MoO_3 with a gas

Table 1. Average Particle Size of H_2 -Reduced MoO_3

Sample	Particle size Å	Surface area/ $\text{m}^2 \text{ g}^{-1}$	
		Calcd	Measured
$\text{MoO}_3(60)$	272	34	67
$\text{MoO}_3(300)$	340	27	170
$\text{MoO}_3(600)$	388	24	180

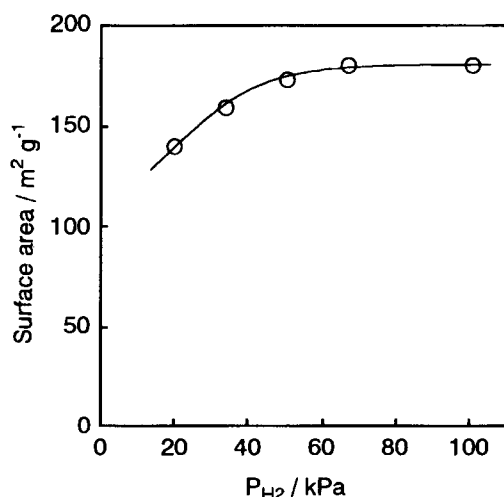


Fig. 5. Effect of partial pressure of H₂ on the surface area of MoO₃ reduced for 12 h at the H₂ flow rate of 600 ml min⁻¹ g⁻¹.

mixture of H₂ and CH₄.¹⁹ Figure 5 shows the surface area of reduced MoO₃ as a function of the partial pressure of H₂. Here, the flow rate of H₂ was adjusted to be 600 ml min⁻¹ g⁻¹. The surface area was slightly dependent on the partial pressure of H₂. Reduction with a gas mixture of 20% H₂ and 80% N₂, however, yielded MoO_x with a surface area of 140 m² g⁻¹, indicating that the effect of the concentration gradient of H₂ was small.

The presence of H₂O vapor has been shown to cause hydrothermal sintering.²⁰ The most likely reason for the positive effect of the reactive gas flow rate on the surface areas of Mo₂N and Mo₂C was suggested by Oyama and co-workers:¹⁹ The H₂O vapor produced by reduction was rapidly removed from the vicinity of MoO₃ particles, and its partial pressure was lowered at a large flow rate of reactive gas, leading to a suppression of sintering. Figure 6 shows the stability of H₂-reduced MoO₃ (600) in the presence of H₂O vapor. A treatment at 623 K in a pure N₂ atmosphere had no effect on

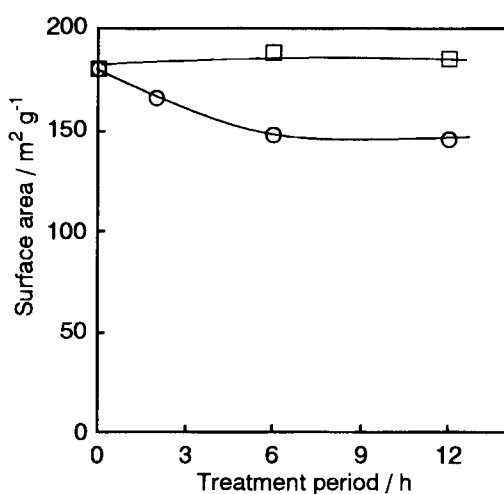


Fig. 6. Stability of the H₂-reduced MoO₃ (600) in the presence of H₂O. The reduced MoO₃ was treated at 623 K in N₂ (□) and in N₂ + H₂O (1226 Pa) (○).

the surface area of MoO₃ (600). When treated in a stream of the N₂-H₂O gas mixture ($P_{H_2O} = 1226$ Pa), the surface area declined. After a treatment for 12 h, the MoO₃ (600) exhibited a surface area of 150 m² g⁻¹. This result indicates that a high surface area can be retained even in the presence of H₂O.

In order to study the effect of H₂O on the formation of MoO_x with a large surface area, reduction was performed in the presence of H₂O vapor. The surface area and average oxidation state of Mo as a function of the partial pressure of H₂O are shown in Fig. 7. The MoO₃ (600) reduced at P_{H_2O} of 1226 Pa exhibited a surface area of 8 m² g⁻¹. This value is almost identical with that of the parent MoO₃. The surface area was enlarged from 8 to 180 m² g⁻¹ by a decrease in P_{H_2O} from 1226 Pa to zero. The Langmuir isotherm gave a better fit of N₂ adsorption data on the MoO₃ with a surface area larger than 100 m² g⁻¹ than the BET isotherm. These results indicate the significant effect of H₂O vapor on the surface area and the formation of micropores. Figure 8 illustrates the XRD patterns of MoO₃ (600) reduced in the presence of H₂O. The diffraction peaks corresponding to MoO₃ were mainly detected in MoO₃ reduced at P_{H_2O} of 1226 Pa. The reduction of MoO₃ was promoted by decreasing P_{H_2O} . The diffraction lines corresponding to the MoO₃ phase disappeared completely, and those of the MoO₂ phase were mainly observed after reduction at P_{H_2O} of 320 Pa. As shown in Fig. 7, the average oxidation state of Mo was lowered by decreasing P_{H_2O} . This is in good agreement with the XRD results. There was a relationship between the surface area and the degree of reduction. This relationship is very similar to that described in Fig. 1. We suggest from these results that the H₂O vapor produced by reduction suppressed the reduction of MoO₃, resulting in the formation of a product with a small surface area.

The reduction of oxide to metal is thermodynamically re-

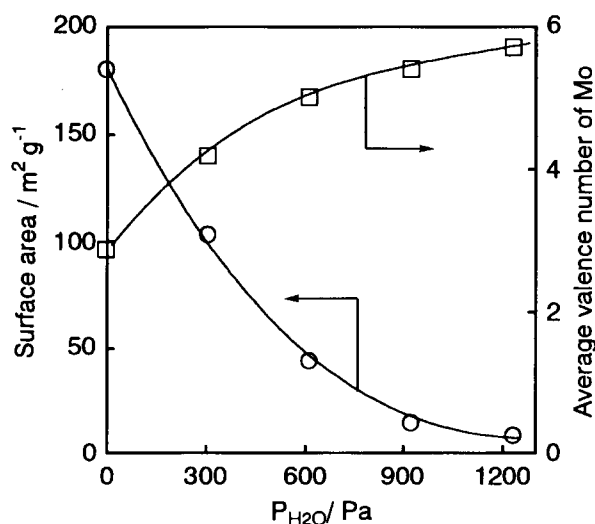


Fig. 7. Effect of partial pressure of H₂O on the surface area (○) and the average valence number of Mo (□). MoO₃ was reduced at 623 K for 12 h in a stream of H₂ (600 ml min⁻¹ g⁻¹).

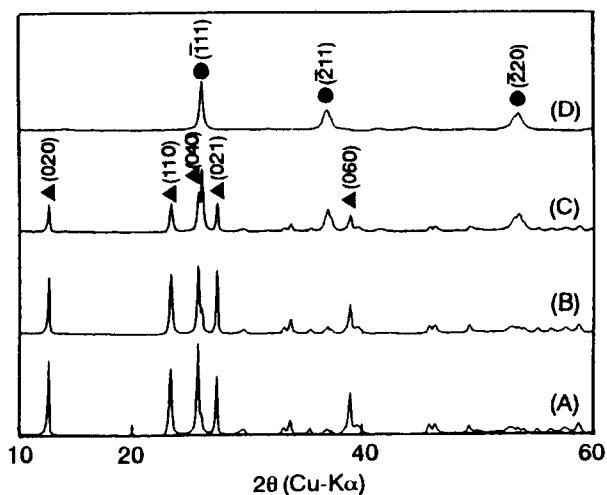


Fig. 8. XRD patterns of MoO_3 (600) reduced with H_2 at 623 K for 12 h in the presence of H_2O . Partial pressure of H_2O : (A), 1226 Pa; (B), 920 Pa; (C), 614 Pa; (D), 320 Pa. ▲, MoO_3 ; ●, MoO_2 .

stricted in the presence of H_2O . The equilibrium constant for the H_2 reduction of MoO_3 to Mo metal at 623 K was calculated to be 2.6×10^4 from thermodynamic data. Therefore, the reduction of MoO_3 to Mo metal can not be thermodynamically limited at this temperature, even in the presence of large amounts of H_2O . Figure 9 shows the average valence number of Mo as a function of the reduction period. Here, MoO_3 was reduced at a H_2 flow rate of $600 \text{ ml min}^{-1} \text{ g}^{-1}$. MoO_3 reduced for 2 h with pure H_2 had an average Mo valence number of 3.9. A H_2 treatment for a longer period gradually lowered the average valence number of Mo, which became 2.7 after reduction for 48 h. The reduction of MoO_3 proceeded progressively with increasing the reduction period, even in the presence of H_2O ($P_{\text{H}_2\text{O}} = 614 \text{ Pa}$). When compared at a definite reduction period, however, the MoO_3 reduced in the presence of H_2O exhibited a larger average valence number of Mo than the MoO_3 reduced with pure H_2 .

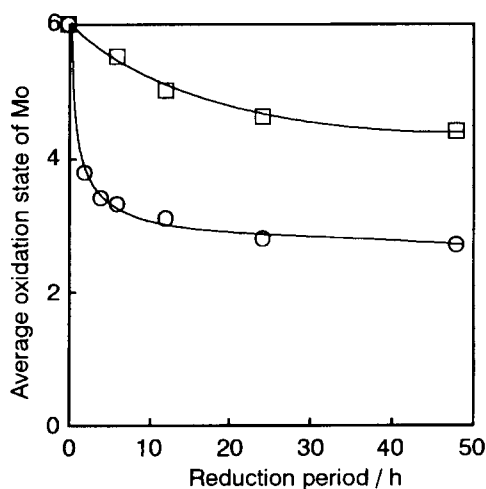


Fig. 9. Average valence number of Mo in the H_2 -reduced MoO_3 (600) as a function of the reduction period. ○, H_2 ; □, $\text{H}_2 + \text{H}_2\text{O}$ (614 Pa).

It is obvious from these results that reduction of MoO_3 can be kinetically controlled in the presence of H_2O .

The effects of the reduction period on the surface area of the reduced MoO_3 are shown in Fig. 10. Under a pure H_2 atmosphere, the reduction of MoO_3 markedly enhanced the surface area, which reached a constant value of $180 \text{ m}^2 \text{ g}^{-1}$ after reduction for 12 h. The surface area of MoO_3 reduced in the presence of H_2O vapor was also dependent on the period of reduction. The degree of enlargement in the presence of H_2O , however, was much small compared with that in pure H_2 . MoO_3 reduced for 48 h in the presence of H_2O exhibited a surface area of $62 \text{ m}^2 \text{ g}^{-1}$. The BET isotherm gave a better fit of N_2 adsorption data on this sample than the Langmuir isotherm, indicating no formation of micropores. Figure 11 shows the relationship between the average valence number of Mo and the surface area. The surface area of H_2 -reduced MoO_3 was highly related to the average valence number of

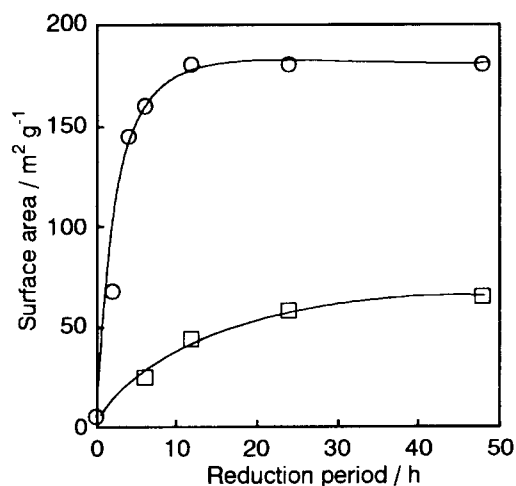


Fig. 10. Surface area of the H_2 -reduced MoO_3 (600) as a function of the reduction period. ○, H_2 ; □, $\text{H}_2 + \text{H}_2\text{O}$ (614 Pa).

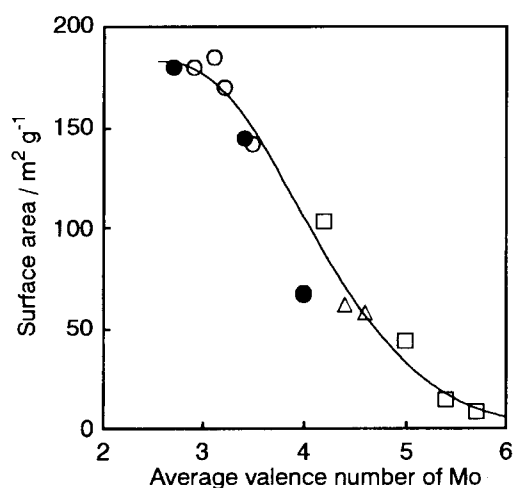


Fig. 11. Relation between the average valence number of Mo and the surface area. Variable: ○, flow rate of H_2 ; □, partial pressure of H_2O ; △, reduction period in the presence of H_2O ; ●, reduction period in pure H_2 .

Mo, irrespective of the reduction conditions, such as the flow rate of H₂, the partial pressure of H₂O, and the reduction period. We conclude on the basis of these experimental results that the surface area and porosity of H₂-reduced MoO₃ was dependent on the degree of reduction.

Conclusion

The H₂ reduction of MoO₃ at 623 K yielded MoO_x with a large surface area. A change in the surface area was induced when the reduction condition differed only in the flow rate of H₂. The surface area increased in proportion to the flow rate of H₂, and reached a constant value of about 180 m² g⁻¹ at a flow rate of H₂ greater than 600 ml min⁻¹ g⁻¹. The MoO_x was a mixture of MoO₂, H_xMoO₃, and MoO_xH_y phases. Although H₂ reduction of MoO₃ produced MoO₂ particles with a smaller size, the large surface area of reduced MoO₃ can not be explained by the particle size. An enlargement of the surface area was accompanied by the formation of micropores, of which the diameter was in the range from 6 to 30 Å. The microporous MoO_x with large surface area was stable at 623 K, even in the presence of H₂O. The degree of reduction and the surface area were lowered by an increase in the partial pressure of H₂O in the reduction process. There was a good relationship between the surface area and the average valence number of Mo, irrespective of the reduction conditions, such as the flow rate of H₂, the partial pressure of H₂O and the reduction period. We conclude from these results that the reduction of MoO₃ to porous MoO_x with a large surface area was prohibited by the action of H₂O produced by the reduction.

This work was supported in part by a Grant-in-Aid for Encouragement of Young Scientists and for Scientific Research on Priority Area A of New Protium Function (No. 299) from the Ministry of Education, Science, Sports and Culture.

References

- 1 C. T. Kresge, M. E. Leonowicz, W. J. Roth, J. C. Vartuli, and J. S. Beck, *Nature*, **359**, 710 (1992).
- 2 J. S. Beck, J. C. Vartuli, W. J. Roth, M. E. Leonowicz, C. T. Kresge, K. D. Schmitt, C. T. W. Chu, D. H. Olson, E. W. Sheppard, S. B. McCullen, J. B. Higgins, and J. L. Schlenka, *J. Am. Chem. Soc.*, **114**, 10834 (1992).
- 3 Z. R. Tian, W. Tong, J. Y. Wang, N. G. Duan, V. V. Krishnan, and S. L. Suib, *Science*, **276**, 926 (1997).
- 4 P. Yang, D. Zhao, D. I. Margolese, B. F. Chmelka, and G. D. Stucky, *Nature*, **396**, 152 (1998).
- 5 A. Katrib, P. Leflaive, L. Hilaire, and G. Maire, *Catal. Lett.*, **38**, 95 (1996).
- 6 A. Katrib, V. Logie, N. Saurel, P. Wehrer, L. Hilaire, and G. Maire, *Surface Sci.*, **337–379**, 754 (1997).
- 7 T. Matsuda, H. Shiro, H. Sakagami, and N. Takahashi, *Catal. Lett.*, **47**, 99 (1997).
- 8 T. Matsuda, Y. Hirata, H. Sakagami, and N. Takahashi, *Chem. Lett.*, **1997**, 1261.
- 9 T. Matsuda, Y. Hirata, S. Suga, H. Sakagami, and N. Takahashi, *Appl. Catal. A General*, **193**, 185 (2000).
- 10 T. Matsuda, Y. Hirata, H. Itoh, H. Sakagami, and N. Takahashi, to be submitted.
- 11 T. Matsuda, Y. Hirata, M. Suzuki, H. Sakagami, and N. Takahashi, *Chem. Lett.*, **1999**, 873.
- 12 P. Delporte, F. Meunier, C. P. Huu, P. Vennegues, M. J. Ledoux, and J. Guille, *Catal. Today*, **23**, 251 (1995).
- 13 L. Volpe and M. Boudart, *J. Solid State Chem.*, **59**, 332 (1985).
- 14 J. G. Choi, R. L. Curl, and L. T. Thompson, *J. Catal.*, **146**, 218 (1994).
- 15 Y. Sato, D. Imai, A. Sato, S. Kasahara, K. Omata, and M. Yamada, *Sekiyu Gakkaishi*, **37**, 514 (1994).
- 16 J. S. Lee, S. T. Oyama, and M. Boudart, *J. Catal.*, **106**, 125 (1987).
- 17 J. S. Lee, L. Volpe, F. H. Ribeiro, and M. Boudart, *J. Catal.*, **112**, 44 (1988).
- 18 E. J. Markel and J. W. Van Zee, *J. Catal.*, **126**, 643 (1990).
- 19 S. T. Oyama, J. C. Schlatter, J. E. Metcalf, and J. M. Lamberg, *Ind. Eng. Chem. Res.*, **27**, 1639 (1988).
- 20 R. F. Horlock, P. L. Morgan, and P. J. Anderson, *Trans. Faraday Soc.*, **59**, 721 (1963).

1 C. T. Kresge, M. E. Leonowicz, W. J. Roth, J. C. Vartuli,